Momentum-kick model description of the ridge in $\Delta\phi$-$\Delta\eta$ correlations in pp collisions at 7 TeV

Cheuk-Yin Wong
Physics Division, Oak Ridge National Laboratory, Oak Ridge, Tennessee 37831, USA
(Received 31 May 2011; published 5 August 2011)

The near-side ridge structure in the $\Delta\phi$-$\Delta\eta$ correlation observed by the CMS Collaboration for pp collisions at 7 TeV at the Large Hadron Collider can be explained by the momentum kick model in which the ridge particles are medium partons that suffer a collision with the jet and acquire a momentum kick along the jet direction. Similar to the early medium parton momentum distribution obtained in previous analysis for nucleus-nucleus collisions at $\sqrt{s_{NN}} = 0.2$ TeV, the early medium parton momentum distribution in pp collisions at 7 TeV exhibits a rapidity plateau as arising from particle production in a flux tube.

DOI: 10.1103/PhysRevC.84.024901 PACS number(s): 25.75.Gz

I. INTRODUCTION

Recently at the Large Hadron Collider (LHC), the CMS Collaboration observed a $\Delta\phi$-$\Delta\eta$ correlation in pp collisions at 7 TeV [1] and in PbPb collisions at $\sqrt{s_{NN}} =$ 2.76 TeV [2], where $\Delta\phi$ and $\Delta\eta$ are the azimuthal angle and pseudorapidity differences of two produced hadrons, respectively. The correlation appears in the form of a "ridge" that is narrow in $\Delta\phi$ at $\Delta\phi \sim 0$ and $\Delta\phi \sim \pi$ but relatively flat in $\Delta\eta$. Similar ridge structures have been observed previously in high-energy nucleus-nucleus AA collisions at the Relativistic Heavy Ion Collider (RHIC) by the STAR Collaboration [3–18], the PHENIX Collaboration [19–23], and the PHOBOS Collaboration [24], with or without a high-p_T trigger [4,16,18].

The CMS observation of the ridge in pp and PbPb collisions raise many interesting questions. How do the ridges arise in pp and AA collisions? Can the ridges in pp and PbPb collisions at LHC and in AA collisions at RHIC be described by the same physical phenomenon? If so, what are the similarities and differences? Why is the ridge yield greatest at $1 < p_T < 3$ GeV/c? What interesting physical quantities do the ridge data reveal? How are the ridges associated with a high-p_T trigger related to the ridges associated with the minimum-bias pair correlation with no high-p_T selection?

Although many theoretical models have been proposed to discuss the ridge phenomenon in AA collisions [25–49] and pp collisions [49–62], the ridge phenomenon has not yet been fully understood. Most of the models deal only with some fragmented and qualitative parts of the experimental data. The most successful quantitative comparisons with experimental data have been carried out in the momentum kick model for the extensive sets of triggered associated particle data of the STAR Collaboration, the PHENIX Collaboration, and the PHOBOS Collaboration: over large regions of p_t, $\Delta\eta$, and $\Delta\phi$ phase spaces and in many different phase space cuts and p_T combinations, including dependencies on centralities, dependencies on nucleus sizes, and dependencies on collision energies [25–27]. As it has been tried and tested successfully for AA collisions at RHIC in previous analyses from which a wealth of relevant pieces of information have been obtained, it is of interest to examine whether the momentum kick model can describe the CMS pp data at 7 TeV to provide answers to the interesting questions we have just posed.[1]

We shall first review the qualitative description of the momentum kick model in Sec. II. We provide additional support for the model in Sec. III by showing how the momentum kick model can explain many peculiar and puzzling features in the minimum-bias correlation data of the STAR Collaboration [4,16,18]. We then summarize the quantitative contents of the model in Sec. IV. The determination of the centrality dependence of the ridge yield necessitates the evaluation of the number of kicked medium particles along the jet trajectory, which we describe in Sec. V. Section VI provides the numerical analysis of the ridge yield and the total associated particle distribution in pp collisions at 7 TeV for comparison with the CMS data. In Sec. VII, we provide answers to the questions posed in the Introduction concerning the ridge phenomena in pp and AA collisions.

II. QUALITATIVE DESCRIPTION OF THE MOMENTUM KICK MODEL

Soon after the observation of the ridge effect in RHIC collisions, a momentum kick model was presented to explain the phenomenon [25–31]. In addition to providing a semiquantitative explanation of experimental data over large regions of p_t, $\Delta\eta$, and $\Delta\phi$ phase spaces in STAR, PHENIX, and PHOBOS experiments, the model serves the useful purposes of identifying and extracting important physical quantities that are otherwise difficult to measure.

To understand the physics of the ridge phenomenon, our first task is to ascertain what the correlated particles are. We need to specify the identities of the correlated particles for the case with a high p_t trigger as well as the minimum-(p_T)-bias trigger without a high-p_T selection. For both cases the two detected particles are correlated in narrow azimuthal angles at $\Delta\phi \sim 0$ or at $\Delta\phi \sim \pi$, relative to each other. Such an experimental observation suggests that the correlated trigger

[1]Based in part on a talk presented at the Workshop on High-pT Probes of High-Density QCD at the LHC at Palaiseau, France, May 30–June 1, 2011.

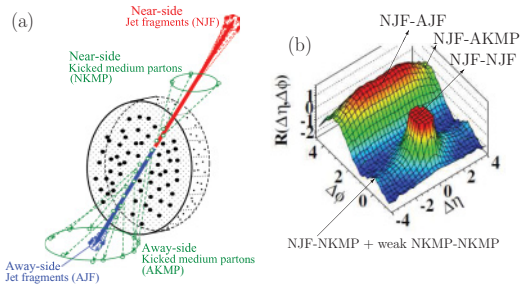

FIG. 1. (Color online) (a) Schematic representation of the momentum kick model. A jet pair (represented by thick arrows) occur back-to-back in a dense medium created in the collision. The jets collide with medium partons, lose energy, and fragment into near-side jet fragments (NJF) and away-side jet fragments (AJF). The near-side kicked medium partons (NMKP) and away-side kicked medium partons (AMKP) (represented by open circular points) that are kicked by the jets acquire a momentum kick along the jet directions and become correlated with the jets at $\Delta\phi \sim 0$ and $\Delta\phi \sim \pi$ as associated "ridge" particles. (b) The CMS data for high-multiplicity pp collisions at 7 TeV [1]. Different regions of the $\Delta\phi$-$\Delta\eta$ correlations may be identified as correlations of different particles associated with the jet fragments (JF) or kicked medium partons (KMP).

and associated particles are related by a collision [25]. It is natural to consider in the momentum kick model the collisions of jets with medium partons (MP) and attribute the ridge as arising from direct jet-(medium parton) collisions. Other models attribute the narrow $\Delta\phi$ correlations to other effects, and future investigations need to sort out the different consequences in quantitative comparison with experiment. Whatever the proposed mechanism may be, collisions of the jet with the medium partons are bound to occur, and the collisional correlation between the colliding objects as discussed in the momentum kick model must be taken into account.

In pp and AA collisions at high energies, pairwise back-to-back jets are produced by the hard-scattering process. These jets encounter the dense medium that is also created in the collision. The jet that encounters less medium material is called the near-side jet. The other jet that encounters more medium material is the away-side jet, as depicted in Fig. 1(a). These two jets collide with medium partons, lose energy, and subsequently break up into jet fragments (JF) in the form of two narrow back-to-back angular cones. The breakup of the near-side jet occurs most likely outside the medium. The away-side jet is quenched. The location of the breakup of the away-side jet, if it is not completely quenched, depends on the degree of its quenching inside the dense medium. The medium partons have an initial momentum distribution at the moment of jet-(medium parton) collision. The kicked medium partons (KMP) that are kicked by a jet acquire a momentum kick along the jet direction. Subsequently, these kicked medium particles materialize as associated "ridge" particles to become correlated with the jets in the $\Delta\phi \sim 0$ and $\Delta\phi \sim \pi$ directions. The momentum distribution of the kicked medium particles is given by the initial momentum distribution displaced by the momentum kick. As a consequence, four types of particles are related to jet-(medium parton) collisions. They are near-side and away-side JF and near- and away-side KMP, as shown in Fig. 1(a).

In our attempt to identify the nature of the correlated particles, it is important to realize that the observed correlation signals refer to those above an uncorrelated background, and the $\Delta\phi \sim 0$ and $\Delta\phi \sim \pi$ correlations place severe restrictions which are satisfied only by causally related particles. One can pick any two particles at random. If both particles arise from the bulk medium that are not related by collisions from the same jet pair as depicted in Fig. 1, the two-particle correlation will show up as a smooth background in $\Delta\phi$. Such a smooth background has been subtracted from our consideration. The remaining correlation arises only from the portion of particles that are causally related by jet-(medium parton) collisions from the *same* pair of back-to-back jets.

Accordingly, we shall identify the two correlated particles as two of the four types of particles shown in Fig. 1(a). In the case with a triggered high-p_T jet particle, the triggered particle of the $\Delta\phi$-correlated pair can be identified as a near-side jet fragment (NJF). The other correlated particle can come from one of four possibilities:

(i) NJF-NJF correlation
If the other particle is also a near-side jet fragment (NJF) from the fragmentation of the same near-side jet, they will be correlated in a cone at ($\Delta\phi \sim 0$, $\Delta\eta \sim 0$).

(ii) NJF-NKMP correlation
If the other particle is a near-side kicked medium parton (NKMP), the other particle will be distributed according to its initial momentum distribution displaced by the momentum kick. If the initial momentum distribution of the medium partons has a rapidity plateau, it will show up as a ridge along $\Delta\eta$ at $\Delta\phi \sim 0$.

(iii) NJF-AKMP correlation
If the other particle is an away-side kicked medium parton (AKMP), this particle will be distributed according to its initial momentum distribution displaced by the momentum kick. If the initial momentum distribution of the medium partons has a rapidity plateau, the kicked medium partons will show up as a ridge along $\Delta\eta$ at $\Delta\phi \sim \pi$. As there are more kicked medium partons on the away side than the near side, the ridge yield will be greater on the away side than the ridge yield on the near side. Because of the additional final-state interactions after the medium partons are kicked, the $\Delta\phi$ and $\Delta\eta$ distributions are expected to be broadened. The degree of $\Delta\phi$ and $\Delta\eta$ broadening increases with the size of the colliding objects.

(iv) NJF-AJF correlation
If the other particle is a member of the away-side jet fragments (AJF), it will show up as a ridge along $\Delta\eta$ at $\Delta\phi \sim \pi$. This $\Delta\eta$ ridge arises from the longitudinal momentum difference of the colliding partons that produce the pair of transverse jets in the hard-scattering process. Clearly, because of the multiple collisions with medium partons as the away-side jet passes through the medium, the jet becomes more broadly distributed in azimuthal and pseudorapidity angles. As a consequence, the away-side jet fragments AJF that

are correlated with the near-side jet have a broader distribution in $\Delta\phi$ and $\Delta\eta$, and a lower average transverse momentum. The strength of the NJF-AJF correlation will also be substantially quenched. The degree of broadening and quenching increases with the size of the colliding objects.

The $\Delta\phi$-$\Delta\eta$ correlation observed in pp collisions at 7 TeV by the CMS Collaboration contains these distinct features listed above in high-multiplicity events, as indicated in Fig. 1(b).

It is important to note that the fragmentation of the degraded near-side jet produces not only high-p_t jet fragments but also low-p_t jet fragments. Evidence of the occurrence of low-p_T jet fragments in the fragmentation of a jet comes from a careful analysis of the two-particle correlation function of associated particle pairs down to p_t as low as 2–3 GeV/c [19]. From the angular cones of these particles as a function of the p_t of the correlated pair, one obtains useful systematics on the jet fragments as a function of p_t [29] [see Eqs. (7), (8), and (9) below]. As p_T of the jet fragment decreases, the jet fragment number $\langle N_{\rm JF}\rangle$ and the jet fragment temperature $T_{\rm JF}$ decreases, but the jet cone angular width of the jet fragments increases. The jet fragment number remains finite down to very low p_T, (even down to $p_T \to 0$) in the systematics. Another piece of evidence for the occurrence of low-p_T jet fragments comes from the minimum-bias pair correlation measurements in STAR [4,16,18] where it was found that there are clusters of low-p_T particles that are located at ($\Delta\phi \sim 0$, $\Delta\eta \sim 0$) in excess of the background. These correlations arises from the fragmentation of a parent jet along the axis of the cone of these correlated pairs.

It should also be realized that the process of fragmentation of a near-side jet occurs most likely outside the medium as depicted in Fig. 1(a). These low p_T particles are subject to no additional final-state interactions with the medium. Furthermore, being kicked out of the dense interacting medium by the jet, the kicked medium partons will also be subject to no additional final-state interactions with the dense medium. Both the jet fragments and kicked medium partons can, therefore, preserve their correlations when they reach the detectors, resulting in the correlation structures as observed.

Because jet fragments can occur with both high and low p_T values, we shall generalize the concept of a jet-fragment "trigger" to include jet fragments of all p_T, both a high-p_T trigger and a minimum-(p_T)-bias trigger. As a minimum-bias trigger contains no selection in p_T, both low-p_T and high-p_T triggers are possible for a minimum-bias trigger. Jet fragments from the same jet correlate with other jet fragments as part of a greater parent jet, no matter what the p_t values of these two jet fragments may be. They are the indicators of the presence of a parent jet. As indicators of a jet, they can be used as reference markers to probe the correlation of other particles that have made collisions with the jet. By using such a generalized concept of "triggered" jet particles of all p_T, the momentum kick model unifies the description of the observed "high-p_T triggered" ridge and the "minimum-(p_T)-bias" ridge (which is sometimes also called soft ridge). It is not necessary to be a high-p_T particle to indicate the presence of a jet, low-p_T particles can also be a jet fragment and indicates the presence of a jet along the p_T direction, when they are used as correlation anchors to measure jet effects on other particles.

In spite of these similarities, there is, however, a notable difference in (i) the case of a high-p_T trigger and (ii) the case of a minimum-bias trigger with no high-p_T selection. In the first case with a high-p_T trigger, it is reasonable to take this trigger particle as a near-side jet fragment (NJF), and the near-side correlations come from its coincidence with another NJF or with a KMP. The correlation contains the NJF-NJF, NJF-NKMP, NJF-AKMP, and NJF-AJF contributions as itemized above.

In the second case of a minimum-bias trigger with a minimum-bias in p_T selection, one of the two correlated pair particles can be taken as a "trigger" and the other as the associated particle. If this trigger particle comes from an NJF, the case of identifying this particle as a jet fragment of all p_T has already been considered and all earlier considerations apply. On the other hand, in the case of a minimum-bias trigger with no bias in high-p_T selection, low-p_T triggers are possible and the low-p_T trigger can be an NKMP. Therefore, correlated with this NKMP trigger, there can be additional NKMP-NKMP, NKMP-AKMP, and NKMP-AJF contributions to the pair correlations for a minimum-bias trigger which we shall list below.

(i) NKMP-NKMP correlation

The associated particle can be a NKMP. There is thus an additional NKMP-NKMP contribution coming from the correlation of two near-side medium partons kicked by the same jet. Each of the kicked medium partons will lie within a small range of ϕ from the jet and therefore the two partons themselves will be correlated relative to each other, with $\Delta\phi \sim 0$. If the initial momentum distribution of the medium partons has a rapidity plateau, the NKMP-NKMP correlations will show up at $\Delta\phi \sim 0$ as a ridge along $\Delta\eta$ whose range is twice as long as the ridge in the NJF-NKMP correlation.

(ii) NKMP-AKMP correlation

The associated particle can be an AKMP. There is an additional NKMP-AKMP contribution to the two-particle correlation coming from the correlation of two medium partons kicked by a near-side jet and an away-side jet of the same hard scattering. The two kicked partons will be correlated relative to each other with $\Delta\phi \sim \pi$. If the initial momentum distribution of the two kicked partons has a rapidity plateau, then the NKMP-AKMP correlation will show up as a ridge along $\Delta\eta$ at $\Delta\phi \sim \pi$ with a range that is twice as long as the ridge in the NJF-NKMP correlation. The correlation may be attenuated and broadened because of the additional final-state interactions suffered by the AKMP after it is kicked by the away-side jet.

(iii) NKMP-AJF correlation

If the low-p_T trigger is a near-side kicked medium parton and if the away-side jet is not completely

quenched, the associated particle can be an AJF. There is the additional NKMP-AJF contribution that shows up as a ridge along $\Delta\eta$ at $\Delta\phi \sim \pi$.

From the above analysis, we can understand the relationship between the correlations in the case with a high-p_T trigger and in the case of a minimum-bias trigger. If we consider the near side, the case with a high-p_T trigger involves mainly NJF-NJF and NJF-NKMP correlations for which the momentum kick model has been successfully applied to explain the near-side data of the STAR, PHENIX, and PHOBOS Collaborations [25–31]. The case with a minimum-bias trigger involves not only these NJF-NJF and NJF-NKMP correlations but also additional NKMP-NKMP correlations. The NKMP-NKMP correlations will contribute only when more than one medium partons are kicked by the same jet and will be important in the ridge region. In extended dense medium as occurs in heavy-ion collisions, the number of partons kicked by the same jet becomes considerable and this NKMP-NKMP contribution should be appropriately taken into account. However, on the near side in pp collisions, the number of medium partons kicked by the same jet is small, the NKMP-NKMP contribution is small in comparison with the other NJF-NJF and NJF-NKMP contributions, and it can be approximately neglected.

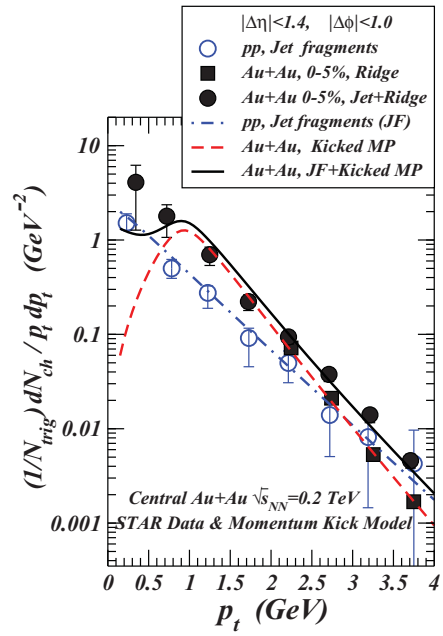

FIG. 2. (Color online) The p_T distribution of associated particles for AuAu collisions at $\sqrt{s_{NN}} = 0.2$ TeV as a function of p_T. The curves are momentum kick model results and the data points are from the STAR Collaboration [3,5].

III. FURTHER SUPPORT FOR THE MOMENTUM KICK MODEL FROM STAR MINIMUM-BIAS PAIR CORRELATION DATA

In addition to the pair correlation measurements with a high-p_T trigger [3,5], the STAR Collaboration has made pair correlation measurements for the case with a minimum-bias trigger, with no high-p_T selections [4,16,18]. The minimum-bias pair correlation data and the related single-particle p_T spectrum contain many peculiar and puzzling features that have so far defied theoretical explanations. In the momentum kick model, these features, however, find simple explanations which provide additional support for the approximate validity of the momentum kick model, as indicated below:

(a) In the case with a minimum-bias trigger with no high-p_T selections, as in the STAR measurements in Refs. [4,16, 18,54,55,63,64], the pair correlations include the NJF-NJF, NJF-NKMP, and NKMP-NKMP correlation components on the near side, and the NJF-AJF, NJF-AKMP, NKMP-AKMP, and NKMP-AJF correlation components on the away side, as explained in the last section.

(b) In the momentum kick model for AuAu collisions at $\sqrt{s_{NN}} = 0.2$ TeV, the peak of the p_T distribution of the medium partons kicked by the near-side jet has been predicted to lie at $p_T \sim 1$ GeV for a high-p_T trigger, as indicated by the dashed curve in Fig. 2 [26–28]. This p_T distribution can be presumed to be also approximately valid for medium partons kicked by the away-side jet. From the relation between the $\Delta\phi$ width and the magnitude of the momentum kick as shown in Fig. 2 of Ref. [25], we envisage further that for the case with a minimum-bias trigger, the undetected underlying parent jet (or back-to-back jets) that give rise to the narrow $\Delta\phi \sim 0$ or $\Delta\phi \sim \pi$ correlations of the kicked medium also provide the same magnitude of the momentum kick to the kicked medium partons. Therefore, the peak of the p_T distribution of the kicked medium partons will also lie at $p_T \sim 1$ GeV/c, for the case of minimum-bias trigger with no p_T selections, on both the near side and the away side. According to the momentum kick model, then, the (p_{T1}, p_{T2}) correlations of the KMP-KMP components on both the near and away sides are expected to center at $p_{T1} \sim p_{T2} \sim 1$ GeV. They correspond to two different kicked medium partons kicked either by the same jet or by a jet and its complementary partner on the other side. They acquire the narrow directional correlation of the ϕ angles from the direction of the jet and the p_T momentum kicks from the same jet or from the separating back-to-back jets. These KMP-KMP correlation components have, indeed, been observed with (y_{t1}, y_{t2}) correlations centering at $y_{t1} \sim y_{t2} \sim 2.8$ corresponding to a (p_{T1}, p_{T2}) correlations centering at $p_{T1} \sim p_{T2} \sim 1$ GeV [4,16,18]. The STAR Collaboration describes this minimum-bias pair correlation structure with various names: the "hard component," the "minijet component" H_0 [4,16,18], or the "pQCD component" [54,55,63,64]. From the momentum kick model points of view, this pair correlation structure arises naturally as the correlation of a pair of medium partons kicked by the same jet on the near side or by a jet and its complementary partner on the other side. The momentum kick model includes these pair correlations as parts of more general multifaceted correlations.

(c) The STAR data indicate the puzzling feature that the (p_{T1}, p_{T2}) pair correlation, centering at $p_T \sim 1$ GeV,

persists as a function of the centrality for both the near-side and the away-side correlations [4,16,18]. This indicates that the detected particles are outside the interaction region of the medium. If they were inside the interaction region, the pair correlation would have been washed out by additional final-state interactions with other medium particles as the medium evolves in time, and the (p_{T1}, p_{T2}) pair correlation will not persist as a function of centrality at the freeze-out point of medium evolution. This peculiar feature is consistent with the KMP-KMP correlation components in the momentum kicked model, where the displacement outside the interaction region arises naturally and early in the medium evolution as the kicked medium partons have been kicked out by the jet (or back-to-back jets) in the jet-(medium parton) collisions. As the charges of the medium partons kicked by the same jet or by back-to-back jets are independent of each other, the (p_{T1}, p_{T2}) pair correlation is the same for the like-sign or unlike-sign pair charges in the momentum kick model, consistent with the STAR observations [16,54].

(d) Being a pair of medium partons kicked by the same jet in the NKMP-NKMP correlation component, the magnitude of the pair correlation structure on the near-side with $\Delta\phi \sim 0$ increases as $N_k(b)[N_k(b) - 1]$, where $N_k(b)$ is the (average) number of medium partons kicked by the jet at the centrality b. Therefore, there is a threshold of this near-side pair correlation component that starts at $N_k(b) \geqslant 2$. As the NKMP parton is now the trigger particle, the yield per trigger increases as $N_k(b)[N_k(b) - 1]/N_k(b)$ and thus increases linearly with $N_k(b) - 1$ after the threshold of $N_k(b) \geqslant 2$, as observed in the behavior of the yield of this pair correlation in the STAR data [4,16,18,54]. The sudden rise of the magnitude of the minimum-bias pair correlation (minijet) on the near side in the STAR data finds a simple explanation.

(e) The NKMP-AKMP correlation component involves a pair of medium partons kicked by a jet and its complimentary partner on the other side with $\Delta\phi \sim \pi$. The magnitude of the pair correlation structure increases as $N_{\rm Nk}(b)N_{\rm Ak}(b)$ where the subscript "Nk" is to indicate that $N_{\rm Nk}(b)$ is the (average) number of medium partons kicked by the near-side jet and the subscript "Ak" is to indicate that $N_{\rm Ak}(b)$ is the (average) number of medium partons kicked by the away-side jet. The momentum kick model predicts that there will not be as sudden a rise of the magnitude of the minimum-bias pair correlation for this NKMP-AKMP correlation component, as compared to the NKMP-NKMP correlation component.

(f) The NJF-KMP as well as the KMP-KMP components contain kicked medium partons that possess their initial momentum distribution before the kick. We envisage that the initial momentum distribution of these medium partons has a rapidity plateau structure and a transverse momentum temperature parameter $T_{\rm MP}$ that is intermediate between those of the jet fragments and the bulk medium. Therefore, the kicked medium partons retain the rapidity plateau structure but a transverse momentum distribution displaced by the momentum kick [25–31]. They show up as a ridge distribution in the $\Delta\eta$ direction in the $\Delta\phi$-$\Delta\eta$ pair correlation, for both the near side and the away side, with the $\Delta\eta$ width much larger than the $\Delta\phi$ width for these components, as observed in the STAR data [4,16,18]. The ridges in the STAR minimum-bias pair correlation ("minijet") data therefore have a simple explanation.

(g) The single-particle distribution will also contain the kicked medium partons, which show up with a thermal-type distribution with a temperature $T_{\rm MP}$ displaced by the momentum kick and centering around $p_T \sim 1$ GeV that differs from the transverse momentum distribution of the bulk unkicked medium partons. The single-particle p_T spectrum therefore contains two components [4,16,18,54]. The kicked medium partons constitute the "hard component," the "minijet H_0 component" [4,16,18], or the "pQCD component" [54,55,63,64] of the single-particle spectrum. Their multiplicities increase with the number of partons kicked by the jet. The mean number of partons kicked by a jet depends on the density of the medium, the jet-(medium parton) cross section, and the path length of the jet passing through the medium, which in turn increases with centrality. Hence, on a per participant pair basis, the magnitude of this "hard" component increases with centrality, as observed in the decomposition of the single-particle spectrum in Refs. [4,16,18,54]. The STAR data indicate that for the most central collision, single-particles from this hard component constitutes a substantial fraction of the total single-particle yield, implying that jet-(medium parton) collisions are important processes governing the spatial and momentum distributions of produced particles in high-energy nuclear collisions.

In summary, the momentum kick model gains additional support by explaining many puzzling features of the pair correlation data in AuAu collisions at $\sqrt{s_{NN}} = 0.2$ TeV obtained by the STAR Collaboration with a minimum-bias trigger. It is, therefore, of interest to examine whether the model can describe the CMS pp data at 7 TeV.

IV. QUANTITATIVE DESCRIPTION OF THE MOMENTUM KICK MODEL

Having presented a qualitative description and supporting evidences for the momentum kick model, we turn now to the quantitative description of the model. To confine the scope of our investigation, we shall limit our attention to correlations on the near side. We shall neglect the NKMP-NKMP contribution, which is a valid consideration for pp collisions that involve only a small number of medium partons kicked by the same jet on the near side.

We briefly summarize the main quantitative contents of the momentum kick model as described in detail in Refs. [25–31]. We follow a jet as it collides with medium partons in a dense medium and study the yield of associated particles for a given $p_t^{\rm trig}$ which has been generalized to include cases of all p_T, as providing an angular location marker for the parent jet.

We label the normalized initial medium parton momentum distribution at the moment of jet-(medium parton) collisions by $E_i dF/d\mathbf{p}_i$. The jet imparts a momentum $\mathbf{q}$ onto a kicked medium parton, which changes its momentum from

$\mathbf{p}_i$ to $\mathbf{p} = (p_t, \eta, \phi) = \mathbf{p}_i + \mathbf{q}$, as a result of the jet-(medium parton) collision. By assumption of parton-hadron duality, the kicked medium partons subsequently materialize as observed associated ridge hadrons.

The normalized final parton momentum distribution $EdF/d\mathbf{p}$ at $\mathbf{p}$ is related to the normalized initial parton momentum distribution $E_i dF/d\mathbf{p}_i$ at $\mathbf{p}_i$ at a shifted momentum, $\mathbf{p}_i = \mathbf{p} - \mathbf{q}$, and we have [25–31]

$$\frac{dF}{p_t dp_t d\eta d\phi} = \left[\frac{dF}{p_{ti} dp_{ti} dy_i d\phi_i}\frac{E}{E_i}\right]_{\mathbf{p}_i=\mathbf{p}-\mathbf{q}} \times \sqrt{1 - \frac{m^2}{(m^2 + p_t^2)\cosh^2 y}}, \quad (1)$$

where the factor E/E_i ensures conservation of particle numbers and the last factor changes the rapidity distribution of the kicked partons to the pseudorapidity distribution [65]. Changing the angular variables to $\Delta\eta = \eta - \eta^{\rm trig}$, $\Delta\phi = \phi - \phi^{\rm trig}$ and characterizing the number of partons kicked by the jet (per jet) by $\langle N_k\rangle$, we obtain the charged ridge particle momentum distribution per trigger jet as

$$\left[\frac{dN_{\rm ch}}{N_{\rm trig} p_t dp_t d\Delta\eta d\Delta\phi}\right]_{\rm ridge} = f_R \frac{2}{3}\langle N_k\rangle \left[\frac{dF}{p_{ti} dp_{ti} dy_i d\phi_i}\frac{E}{E_i}\right]_{\mathbf{p}_i=\mathbf{p}-\mathbf{q}} \times \sqrt{1 - \frac{m^2}{(m^2 + p_t^2)\cosh^2 y}}, \quad (2)$$

where f_R is the average survival factor for produced ridge particles to reach the detector and the factor 2/3 is to indicate that 2/3 of the produced associated particles are charged. Present measurements furnish information only on the product $f_R\langle N_k\rangle$. For pp collisions with a small transverse extent, the kicked medium partons are likely to escape from the interaction region after the kick and f_R can be approximately taken to be unity. The momentum kick $\mathbf{q}$ will be distributed in the form of a cone around the trigger jet direction with an average $\langle\mathbf{q}\rangle = q_L \mathbf{e}^{\rm trig}$ directed along the trigger direction $\mathbf{e}^{\rm trig}$ of the parent jet.

We have extracted the normalized initial medium parton momentum distribution on the right-hand side of Eq. (2) from STAR, PHENIX, and PHOBOS data, we find that the normalized distribution can be represented in the form [26–31]

$$\frac{dF}{p_{ti} dp_{ti} dy_i d\phi_i} = A_{\rm ridge}(1-x)^a \frac{e^{-\sqrt{m_\pi^2 + p_{ti}^2}/T_{\rm MP}}}{\sqrt{m_d^2 + p_{ti}^2}}, \quad (3)$$

where $A_{\rm ridge}$ is a normalization constant, x is the light-cone variable

$$x = \frac{\sqrt{m_\pi^2 + p_{ti}^2}}{m_\pi} e^{|y_i| - y_B}, \quad (4)$$

a is the fall-off parameter, y_B is the rapidity of the beam nucleons in the center-of-mass system, $T_{\rm MP}$ is the medium parton temperature parameter, m_π is the pion mass, and $m_d =$ 1 GeV is to correct for the behavior of the p_T distribution at low p_T as discussed in Refs. [26,28].

The total observed yield of associated particles per trigger consists of the sum of the ridge (NJF-NKMP) component and the jet fragments (NJF-NJF) component,

$$\left[\frac{1}{N_{\rm trig}}\frac{dN_{\rm ch}}{p_t dp_t d\Delta\eta d\Delta\phi}\right]_{\rm total} = \left[\frac{dN_{\rm ch}}{N_{\rm trig} p_t dp_t d\Delta\eta\, d\Delta\phi}\right]_{\rm ridge} + f_J \left[\frac{dN_{\rm jet}^{pp}}{p_t dp_t\, d\Delta\eta\, d\Delta\phi}\right]_{\rm JF}, \quad (5)$$

where f_J is the survival factor of the jet fragments as they propagate out of the medium. For fragmentation outside the medium, as is likely to occur in pp collisions, f_J can be set to unity. The experimental associated jet fragment distribution in pp collisions can be described well by [28]

$$\left[\frac{dN_{\rm JF}^{pp}}{p_t dp_t\, d\Delta\eta\, d\Delta\phi}\right]_{\rm JF} = N_{\rm JF}\frac{\exp\left\{\left(m_\pi - \sqrt{m_\pi^2 + p_t^2}\right)/T_{\rm JF}\right\}}{T_{\rm JF}(m_\pi + T_{\rm JF})} \times \frac{1}{2\pi\sigma_\phi^2} e^{-[(\Delta\phi)^2 + (\Delta\eta)^2]/2\sigma_\phi^2}, \quad (6)$$

where $N_{\rm JF}$ is the total number of near-side (charged) jet fragments associated with the p_T trigger and $T_{\rm JF}$ is the jet fragment temperature parameter. Extensive sets of data from the PHENIX Collaboration give $N_{\rm JF}$ and $T_{\rm JF}$ parameters that vary approximately linearly with $p_t^{\rm trig}$ of the trigger particle for pp collisions at $\sqrt{s_{NN}} = 0.2$ TeV [27],

$$N_{\rm JF} = 0.15 + (0.10/{\rm GeV/c})p_t^{\rm trig}, \quad (7)$$

$$T_{\rm JF} = 0.19\,{\rm GeV} + 0.06 p_t^{\rm trig}. \quad (8)$$

We also find that the width parameter σ_ϕ of the jet fragment cone depends slightly on p_t which we parametrize as

$$\sigma_\phi = \sigma_{\phi 0}\frac{m_a}{\sqrt{m_a^2 + p_t^2}}, \quad (9)$$

where $m_a = 1.1$ GeV.

With the above formulation, the associated particle distribution is written in terms of physical quantities, namely the normalized initial medium parton momentum distribution $E_i dF/d\boldsymbol{p}_i$, the magnitude of the momentum kick q_L, and the number of kicked medium particles $\langle N_k\rangle$ which depends on the centrality of the collision.

V. CENTRALITY DEPENDENCE OF THE RIDGE YIELD

The CMS Collaboration obtained the ridge yield as a function of the charge (particle) multiplicity. It is necessary to determine the centrality dependence of both the ridge yield and the charge multiplicity.

In the momentum kick model, the ridge yield is proportional to the number of kicked medium partons. We showed previously how the (average) number of kicked medium partons per jet, $\langle N_k(\boldsymbol{b})\rangle$, can be evaluated as a function of the

impact parameter $\boldsymbol{b}$ for AA collisions [28,29]. Here, we briefly summarize these results and apply them to pp collisions by treating the colliding protons as extended droplets as in the Chou-Yang model [66].

Accordingly, we examine the collision of two extended objects A and B in Fig. 3 and use the transverse coordinate system with the origin at $\boldsymbol{O}$ that is the midpoint between the two centers, $\boldsymbol{O}_A$ and $\boldsymbol{O}_B$, of the extended objects. In this transverse coordinate system, the location of the jet production point is labeled as $\boldsymbol{b}_0$, measured from the origin $\boldsymbol{O}$. The jet is produced by the collision of a projectile parton and a target parton at $\boldsymbol{b}_0$. The jet production point $\boldsymbol{b}_0$ measured relative to the two nucleon centers $\boldsymbol{O}_A$ and $\boldsymbol{O}_B$ are then given by

$$\boldsymbol{b}_A = \boldsymbol{b}_0 + \boldsymbol{b}/2, \tag{10}$$

$$\boldsymbol{b}_B = \boldsymbol{b}_0 - \boldsymbol{b}/2. \tag{11}$$

From the Glauber model, the probability of finding a target parton at $\boldsymbol{b}_0$ is $T_A(\boldsymbol{b}_A)$, and the probability of finding a projectile parton at $\boldsymbol{b}_0$ is $T_B(\boldsymbol{b}_B)$. The probability for the production of a jet at $\boldsymbol{b}_0$ in the collision of A and B at an impact parameter $\boldsymbol{b}$, $P_{\rm jet}(\boldsymbol{b}_0, \boldsymbol{b})$, is

$$P_{\rm jet}(\boldsymbol{b}_0, \boldsymbol{b}) = \frac{T_A(\boldsymbol{b}_0 + \boldsymbol{b}/2)T_B(\boldsymbol{b}_0 - \boldsymbol{b}/2)}{\int d\boldsymbol{b}_0 T_A(\boldsymbol{b}_0 + \boldsymbol{b}/2)T_B(\boldsymbol{b}_0 - \boldsymbol{b}/2)}, \tag{12}$$

which is normalized as

$$\int d\boldsymbol{b}_0 P_{\rm jet}(\boldsymbol{b}_0, \boldsymbol{b}) = 1. \tag{13}$$

The magnitude of the ridge structure depends on the transverse momentum of the trigger particle. The greater is the transverse momentum of the trigger particle above approximately 10 GeV/c, the less will be the probability for the appearance of the ridge structure [2,19]. There is a dependence of the jet-(medium parton) interaction on the trigger p_T that needs to be further investigated in the future.

In our present work, we shall limit our attention to a parent jet that can interact with medium partons to lead to the ridge structure. This means that the parent jet p_T considered is approximately of order 10 GeV with trigger p_T fragments from low p_T values up to a few GeV/c. We consider the parent jet to traverse on the near side along the trajectory $\boldsymbol{l}$ that is measured from the point of production $\boldsymbol{b}_0$ and points in the ϕ_s direction with respect to the reaction plane, as shown in Fig. 3. The jet will collide with medium partons along its way. We consider one such a collision at the transverse coordinate $\boldsymbol{b}'$ as measured from the origin $\boldsymbol{O}$. The collision point $\boldsymbol{b}'_A$ and $\boldsymbol{b}'_B$ measured relative to the two centers $\boldsymbol{O}_A$ and $\boldsymbol{O}_B$ are then given by

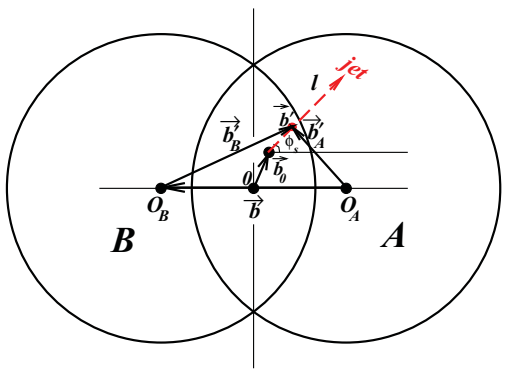

FIG. 3. (Color online) The transverse coordinate system used to calculate the number of kicked medium partons along the jet trajectory in the collision of A and B at an impact parameter $\boldsymbol{b} = \boldsymbol{b}_A - \boldsymbol{b}_B$. The jet source point is $\boldsymbol{b}_0$ and the jet-(medium parton) collision point is $\boldsymbol{b}'$. The jet trajectory lies along $\boldsymbol{l}$ and makes an angle ϕ_s with respect to the reaction plane.

$$\boldsymbol{b}'_A = \boldsymbol{b}' + \boldsymbol{b}/2, \tag{14}$$

$$\boldsymbol{b}'_B = \boldsymbol{b}' - \boldsymbol{b}/2, \tag{15}$$

$$\boldsymbol{b} = \boldsymbol{b}'_A - \boldsymbol{b}'_B. \tag{16}$$

The collision point $\boldsymbol{b}'$ dependence on $\boldsymbol{b}_0$, $\boldsymbol{l}$, and ϕ_s is given by

$$\boldsymbol{b}'(\boldsymbol{b}_0, \boldsymbol{l}, \phi_s) = (b'_x, b'_y) = (b_{0x} + l\cos\phi_s, b_{0y} + l\sin\phi_s), \tag{17}$$

which will be needed later on to evaluate the number of kicked medium partons. We label the number of kicked medium partons per jet as $N_k(\boldsymbol{b}_0, \phi_s, \boldsymbol{b})$. The average of $N_k(\boldsymbol{b}_0, \phi_s, \boldsymbol{b})$ with respect to $\boldsymbol{b}_0$ is

$$\bar{N}_k(\phi_s, \boldsymbol{b}) \equiv \langle N_k(\boldsymbol{b}_0, \phi_s, \boldsymbol{b})\rangle_{\boldsymbol{b}_0} = \frac{\int d\boldsymbol{b}_0 N_k(\boldsymbol{b}_0, \phi_s, \boldsymbol{b}) P_{\rm jet}(\boldsymbol{b}_0, \boldsymbol{b})}{\int d\boldsymbol{b}_0 P_{\rm jet}(\boldsymbol{b}_0, \boldsymbol{b})}. \tag{18}$$

The jet is attenuated along its way, and the attenuation is described by $\exp\{-\zeta N_k(\boldsymbol{b}_0, \phi_s, \boldsymbol{b})\}$ with an attenuation coefficient ζ that depends on the energy loss and the change of the fragmentation function on energy [27]. So when the jet attenuation is taken into account, we get

$$\bar{N}_k(\phi_s, \boldsymbol{b}) \equiv \langle N_k(\boldsymbol{b}_0, \phi_s, \boldsymbol{b})\rangle_{\boldsymbol{b}_0} = \frac{\int d\boldsymbol{b}_0 N_k(\boldsymbol{b}_0, \phi_s, \boldsymbol{b}) e^{-\zeta N_k(\boldsymbol{b}_0, \phi_s, \boldsymbol{b})} P_{\rm jet}(\boldsymbol{b}_0, \boldsymbol{b})}{\int d\boldsymbol{b}_0 e^{-\zeta N_k(\boldsymbol{b}_0, \phi_s, \boldsymbol{b})} P_{\rm jet}(\boldsymbol{b}_0, \boldsymbol{b})}. \tag{19}$$

We further get the average over angle ϕ_s and we get

$$\bar{\bar{N}}_k(\boldsymbol{b}) \equiv \langle N_k(\boldsymbol{b}_0, \phi_s, \boldsymbol{b})\rangle_{\boldsymbol{b}_0, \phi_s} = \frac{1}{\pi/2}\int_0^{\pi/2} d\phi_s \langle N_k(\boldsymbol{b}_0, \phi_s, \boldsymbol{b})\rangle_{\boldsymbol{b}_0}. \tag{20}$$

To proceed further, we need to evaluate $N_k(\boldsymbol{b}_0, \phi_s, \boldsymbol{b})$. The number of jet-(medium parton) collisions along the jet trajectory that originates from $\boldsymbol{b}_0$ and makes an angle ϕ_s with respect to the reaction plane is

$$N_k(\boldsymbol{b}_0, \phi_s, \boldsymbol{b}) = \int_0^\infty \sigma\, dl \frac{dN_{\rm MP}}{dV}(\boldsymbol{b}'_A, \boldsymbol{b}'_B), \tag{21}$$

where $0 < l < \infty$ parametrizes the jet trajectory, σ is the jet-(medium parton) scattering cross section, and $dN_{\rm MP}(\boldsymbol{b}')/dV$ is the medium parton density at $\mathbf{b}'$ along the trajectory $\boldsymbol{l}$. We start the time clock for time measurement at the moment of maximum overlap of the colliding nuclei, and the jet is produced by parton-parton collisions at a time $t \sim \hbar/(10\,{\rm GeV})$ which can be taken to be ~ 0. The trajectory path length l is then a measure of the time coordinate, $t \approx l$. Due to

the longitudinal expansion the density is depleted and the temperature is decreased as [67]

$$T \propto (t_0/t)^{c_s^2}, \tag{22}$$

where c_s is the speed of sound and t_0 is the initial time. As the entropy density and number densities are proportional to T^{1/c_s^2}, the density of the medium partons therefore varies with time t as [67]

$$\frac{dN_{\rm MP}}{dV}(b',t) = \frac{dN_{\rm MP}}{dV}(b',t=t_0)\frac{t_0}{t}. \tag{23}$$

The medium parton density $dN_{\rm MP}/dV$ at $(b'_{\rm init}, t = t_0)$ is related to the parton transverse density $dN_{\rm MP}/d\boldsymbol{b}$ at t_0 by

$$\frac{dN_{\rm MP}}{dV}(b',t=t_0) = \frac{dN_{\rm MP}}{2t_0 d\boldsymbol{b}'}(b',t=t_0). \tag{24}$$

To obtain the medium parton density, we introduce the concept of an extended droplet to describe the proton, as in the Chou-Yang [66] model with the droplet number of a proton normalized to unity. Collisions between droplet elements of one proton and the droplet elements of the other proton leads to the production of medium partons. As in high-energy heavy-ion collision, we assume that the number of medium partons is proportional to the number of participating droplet elements $N_{\rm particp}$ with a proportional constant κ'

$$\frac{dN_{\rm MP}}{dN_{\rm particp}} = \kappa'. \tag{25}$$

The initial parton number transverse density $dN_{\rm MP}/d\boldsymbol{b}'$ at $t = t_0$ is then related to the corresponding participating droplet element transverse density $dN_{\rm MP}/d\boldsymbol{b}'$ as

$$\frac{dN_{\rm MP}}{d\boldsymbol{b}'} = \kappa'\frac{dN_{\rm particp}}{d\boldsymbol{b}'}. \tag{26}$$

We need to evaluate the κ' parameter for pp collision at 7 TeV. Landau hydrodynamical model gives [68–70]

$$N_{\rm ch} = K(\xi\sqrt{s_{NN}}/{\rm GeV})^{1/2}, \tag{27}$$

where $K = 2.019$ and ξ is the fraction of incident energy that goes into particle production in pp and $p\bar{p}$ collisions. An examination of the charge multiplicity in pp and $p\bar{p}$ collisions indicates that the particle production energy fraction ξ is approximately 0.5 for these collisions [71]. So, for pp at 7 GeV, the average charge multiplicity is

$$N_{\rm ch} = 120. \tag{28}$$

To determine κ', we use a sharp-cutoff thickness function of the form for the nucleons (Eq. (12.29) of Ref. [65])

$$T_A(\boldsymbol{b}_A) = \frac{3}{2\pi R_A^3}\sqrt{R_A^2 - b_A^2}\,\Theta(R_A - b_A), \tag{29}$$

which gives an average number of participating droplet elements $\langle N_{\rm particp}\rangle = 0.4894$ and

$$\frac{N_{\rm MP}}{N_{\rm particp}} = \frac{dN_{\rm MP}}{dN_{\rm particp}} = \frac{3}{2}\frac{dN_{\rm ch}}{dN_{\rm particp}} = \kappa' = 367. \tag{30}$$

The transverse participant number density needed in Eqs. (21) and (26) along the jet trajectory can be obtained from the Glauber model to be

$$\frac{dN_{\rm particp}}{d\boldsymbol{b}'}(\boldsymbol{b}'_A, \boldsymbol{b}'_B) = [T_A(\boldsymbol{b}'_A) + T_B(\boldsymbol{b}'_B)]\Theta(\mathcal{R}), \tag{31}$$

where $\Theta(\mathcal{R})$ denotes a step function that is unity inside the overlapping region and zero outside. The number of jet-(medium parton) collisions along the jet trajectory making an angle ϕ_s with respect to the reaction plane is

$$N_k(\boldsymbol{b}_0, \phi_s, \boldsymbol{b}) = \int_0^\infty \frac{\sigma\, dl}{2t_0}\kappa'[T_A(\boldsymbol{b}'_A) + T_B(\boldsymbol{b}'_B)]\Theta(\mathcal{R})\frac{t_0}{t}, \tag{32}$$

where $\boldsymbol{b}'_A$ and $\boldsymbol{b}'_B$ are given in terms of $\boldsymbol{b}_0$, ϕ_s, $\boldsymbol{b}$, and $\boldsymbol{l}$ by Eqs. (14), (15), and (17). This expression allows us to evaluate the number of average kicked medium partons per jet $\bar{\bar{N}}(\boldsymbol{b})$ as a function of the impact parameter.

There is an amendment which need to be taken into account. To produce a medium parton with a transverse mass $m_T \sim p_T$, a period of initial time $t_0 \sim \hbar/p_T$ is, however, needed to convert the longitudinal kinetic energy of the collision into entropy so the jet-MP collision can commence [67]. At RHIC with $\sqrt{s_{NN}} = 0.2$ TeV, the time for producing a particle with a typical transverse mass or transverse momentum of about 0.35 GeV is $\hbar/(0.35{\rm GeV}/c) \sim 0.6\,{\rm fm}/c$, which is also the time estimated for the thermalization of the produced matter [72]. Previous estimates of the jet-MP cross section and attenuation coefficient ζ have been obtained with such a t_0 value. At LHC with $\sqrt{s_{NN}} = 7$ TeV, $\langle p_T\rangle = 0.545\ {\rm GeV}/c$ [73], which is substantially greater than the average transverse momentum in RHIC collisions at $\sqrt{s_{NN}} = 0.2$ TeV. Consequently, we need a smaller value of t_0 for LHC collisions as compared to RHIC collisions.

Equation (32) can be substituted into Eq. (20) to allow the evaluation of the number of ridge particles $\bar{\bar{N}}_k(\boldsymbol{b})$ as a function of the impact parameter b. We also need the relation between the charge multiplicity $N_{\rm ch}(\boldsymbol{b})$ inside the CMS rapidity window as a function of the impact parameter $\boldsymbol{b}$. Using Eqs. (30) and (31), we obtain

$$N_{\rm ch}(\boldsymbol{b}) = C_{\rm CMS}\frac{2}{3}\kappa'\int d\boldsymbol{b}'[T_A(\boldsymbol{b}' + \boldsymbol{b}/2) + T_B(\boldsymbol{b}' - \boldsymbol{b}/2)]\Theta(\mathcal{R}), \tag{33}$$

where $C_{\rm CMS}$ is the fraction of produced particles inside the CMS rapidity window of $-2.4 < \eta < 2.4$. Assuming a rapidity plateau for produced particles, this fraction for the multiplicity of particles, within the CMS rapidity window in pp collisions 7 TeV with $y_B = 8.91$, is

$$C_{\rm CMS} = \frac{({\rm CMS}_{\rm rapidity\ range})}{2y_B} = 0.269. \tag{34}$$

By using these results, we can relate the CMS charge multiplicity $N_{\rm ch}(\boldsymbol{b})$ and the average number of kicked medium partons (per jet) $\bar{\bar{N}}_k(\boldsymbol{b})$.

VI. MOMENTUM KICK MODEL ANALYSIS OF *pp* COLLISIONS AT 7 GEV

Previously, the momentum kick model analyses of STAR, PHENIX, and PHOBOS data yield a wealth of useful information. We learn that the initial momentum distribution is in the form of a rapidity plateau, as in the production of particles in a flux tube [30,65,67,74,75], and the transverse distribution is in the form of a thermal-type distribution with a medium-parton temperature $T_{\rm MP}$. The STAR ridge data at $\sqrt{s_{NN}} = 0.2$ TeV can be described by a MP momentum distribution of the form in Eq. (3) with parameters [26–30]

$$a = 0.5,\ T_{\rm MP} = 0.5\,{\rm GeV},\ \text{ and } m_a = 1{\rm GeV}. \tag{35}$$

The magnitude of the momentum kick per collision, q_L, was found to be 0.8–1 GeV/c. The centrality dependence of the ridge yield can be described by

$$\zeta = 0.20,\ \sigma = 1.4\,{\rm mb},\ t_0 = 0.6\,{\rm fm}/c. \tag{36}$$

For the description of the jet fragments, extensive set of PHENIX data give systematics of the jet fragments as given in Eqs. (7), (8), and (9).

In going from AA collisions at $\sqrt{s_{NN}} = 0.2$ TeV to pp collisions at 7 TeV, there are similarities and obvious differences. The plateau structure of the medium parton distributions in the two cases are expected to be similar, and the extension of the plateau should similarly depend on the beam rapidity y_B as given in Eqs. (3) and (4).

We need to know the size of the proton and how the multiplicity depends on centrality. The extrapolated pp cross section at 7 TeV (PDG, 2010) gives [76],

$$\sigma_{\rm tot}(pp) \sim 110\,{\rm mb},\ \sigma_{\rm elastic} \sim 30\,{\rm mb}. \tag{37}$$

Therefore, the pp inelastic cross section at this energy is

$$\sigma_{\rm inel} \sim 80\,{\rm mb}. \tag{38}$$

Sum of $p+p$ radii in a pp inelastic collision is then

$$R = \sqrt{80\,{\rm mb}/\pi} = 1.59\,{\rm fm} = R_A + R_B. \tag{39}$$

Therefore, each proton has a radius $R_A = 0.8$ fm for inelastic collisions with the production of particles.

There is, however, an important difference between RHIC and LHC that must be taken into account. For CMS data for pp collisions at $\sqrt{s_{NN}} = 7$ GeV [73],

$$\langle p_T \rangle = 0.545\,{\rm GeV}/c. \tag{40}$$

For RHIC collisions at $\sqrt{s_{NN}} = 0.2$ TeV,

$$\langle p_T \rangle = 0.39\,{\rm GeV}/c. \tag{41}$$

Therefore, the average transverse momentum of produced medium particle at 7 TeV is enhanced from the average transverse momentum of produced medium particle at $\sqrt{s_{NN}} =$ 0.2 TeV by the factor

$$\frac{\langle p_T \rangle(7\,{\rm TeV})}{\langle p_T \rangle(0.2\,{\rm TeV})} = \frac{0.545\,{\rm GeV}/c}{0.39\,{\rm GeV}/c} = 1.4. \tag{42}$$

Because of this enhancement in the average p_T values, it is necessary to scale those quantities that are related directly to transverse momentum by this empirical factor of 1.4.

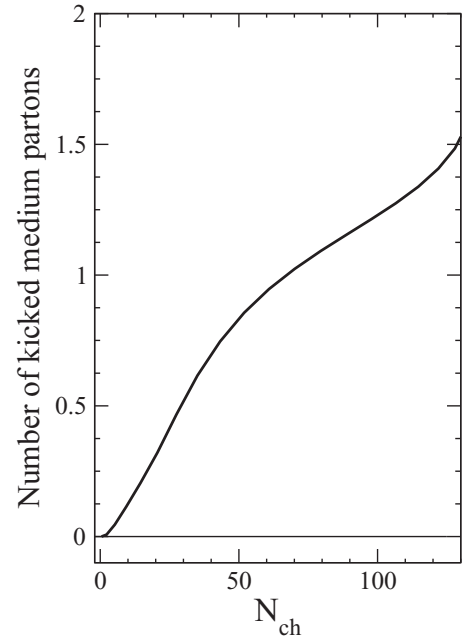

FIG. 4. The number of average kicked medium partons $N_k(\boldsymbol{b})$ per minimum-bias trigger particle as a function of charge multiplicity $N_{\rm ch}(\boldsymbol{b})$.

Accordingly, the relevant parameters that we need to change are the medium parton temperature $T_{\rm MP}$, the jet fragment temperature $T_{\rm JF}$, and the medium parton initial time t_0 which varies roughly as $1/p_T$. For the analysis of CMS data at 7 TeV, we are well advised to scale up $T_{\rm MP}$ and $T_{\rm JF}$ by a factor of 1.4 to result in

$$T_{\rm MP} = 0.7\,{\rm GeV},\quad T_{\rm JF} = 0.266\,{\rm GeV} + 0.084\,p_t^{\rm trig} \tag{43}$$

and reduce the initial time t_0 by a factor of 1.4 to get

$$t_0 = 0.43\,{\rm fm}/c. \tag{44}$$

As a function of the impact parameter, we calculate the average number of kicked medium partons per jet, which gives the ridge yield per jet as in Eq. (2). After calibrating the number of average droplet participants with the average number of produced charged particles as given in Eq. (30), we calculate the charge multiplicity as a function of the impact parameter. These two calculations gives the ridge yield per jet as a function of the charge multiplicity.

The jet trajectory calculation indicates that the average number of kicked partons for the most central pp collision is about 1.5 as shown in Fig. 4. With the parameters properly scaled according to the transverse momenta, the only free parameter is q_L, the magnitude of the momentum kick acquired by the medium parton per jet-MP collision. Previously, for the STAR data at $\sqrt{s_{NN}} = 0.2$ TeV, the magnitude of q_L was found to be 0.8–1.0 GeV/c per kick. We vary q_L to fit the variation of the CMS ridge yield data in different p_T windows. If the magnitude of q_L remains at 1 GeV/c, the ridge yield will be too large in the regions of $0.1 < p_T < 1$ GeV/c and too small in the region $2 < p_T < 3$ GeV/c. The results do not agree with data. It is found that the magnitude of the kick $q_L = 2$ GeV/c gives results that are qualitatively consistent

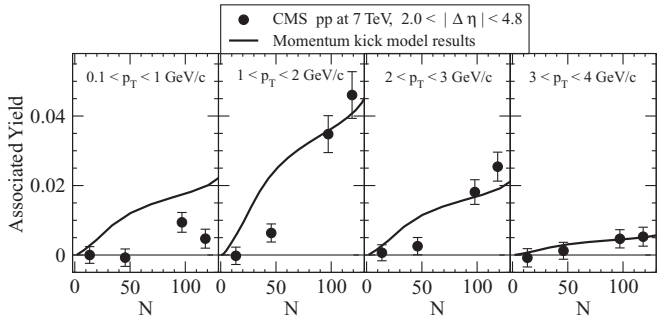

FIG. 5. The ridge yield per minimum-bias trigger particle for different regions of associated particle p_T, as a function of the multiplicity in the interval $2 < |\Delta\eta| < 4.8$; (a) is for $0.1 < p_T < 1$ GeV/c, (b) for $1 < p_T < 2$ GeV/c, (c) for $0.2 < p_T < 3$ GeV/c, and (d) for $3 < p_T < 4$ GeV/c.

with the data. The yield per minimum-bias trigger particle for different regions of associated particle p_T, as a function of the multiplicity, is shown in Fig. 5, where the CMS data are shown as solid points and the momentum kick model results are shown as curves. The general trend of the experimental data is reasonably reproduced by the momentum kick model.

Another indication of the dependence of the angular distribution of the associated particle yield on transverse momentum of the associated particle is shown in Fig. 6, where Fig. 6(a) is for $0.1 < p_T < 1.0$ GeV/c and 5(b) is for $1 < p_T < 3$ GeV/c. These total associated particle yields for the minimum-bias pair correlation has been calculated for a triggered particle with $p_t^{\rm trig} = 0.545$ GeV/c, corresponding to the minimum-bias average p_T of detected hadrons given in Eq. (40). The top of the distributions have been truncated to show the distributions in a finer scale. The ridge structure is almost imperceptible for $0.1 < p_T < 1.0$ GeV/c in Fig. 6(a) but shows up clearly for $1.0 < p_T < 3.0$ GeV/c in Fig. 6(b). The theoretical associated particle yield pattern of the $\Delta\phi$-$\Delta\eta$

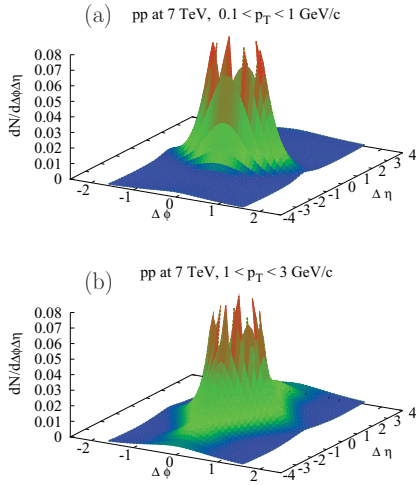

FIG. 6. (Color online) The distribution of associated particles for pp collisions at 7 TeV calculated in the momentum kick model. The peaks of the distributions have been truncated at the top. Figure 5(a) is for $0.1 < p_T < 1$ GeV/c and Fig. 5(b) is for $1 < p_T < 3$ GeV/c.

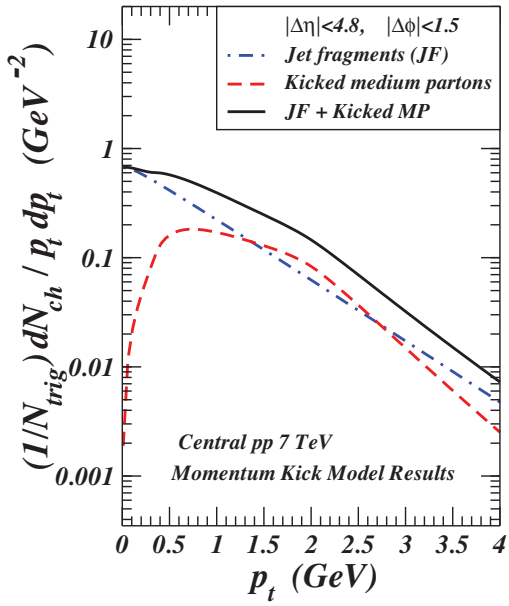

FIG. 7. (Color online) The p_T distribution of associated particles for central pp collisions at 7 TeV obtained in the momentum kick model.

angular distributions as a function of p_T agrees with those observed in CMS experiments.

To exhibit further the dependence of the ridge yield on p_t and collision energy, we note in Fig. 2 that for AuAu collisions at $\sqrt{s_{NN}} = 0.2$ TeV within the acceptance windows of the STAR Collaboration, the ridge yield $dN_{\rm ch}/N_{\rm trig}p_T dp_T$ has a peak at about 1 GeV/c, which is about the same as the magnitude of the momentum kick $q_L = 1$ GeV/c. Because $T_{\rm MP} < T_{\rm JF}$, the NJF-NJF component dominates over the NJF-NKMP components at large p_T.

To make meaningful comparison with pp collisions at 7 TeV, we calculate $dN_{\rm ch}/N_{\rm trig}p_T dp_T$ in the momentum kick model with $q_L = 2$ GeV/c within the CMS experimental windows with a $p_T = 5$ GeV/c trigger. The theoretical results are shown as curves in Fig. 7. The ridge yield distributions are the medium parton distributions displaced by the momentum kick along the jet direction. As a consequence, the peak of the ridge yield (dashed curve) moves to a larger value of p_T and becomes broader over a large region between 0.5 to 2.5 GeV/c for pp collisions at 7 TeV with $q_L = 2$ GeV/c. The large pseudorapidity window for the trigger jet enhances the broadening of the peak of the distribution for pp collisions. These theoretical results explain why the associated particle yield is distributed more in the region of $1 < p_T < 3$ GeV/c than in other regions in pp collisions at 7 TeV. Note again that because the the higher temperature for the NJF-NJF component, the ridge yield become smaller than the NJF-NJF yields as p_T increases above 3 GeV/c.

VII. CONCLUSIONS AND DISCUSSIONS

The CMS observation of the ridge structures in pp collisions at 7 TeV raises many interesting questions which

we can try to answer in the momentum kick model. We find that in AA as well as in pp collisions, the ridge arises from the medium partons that are kicked by the jet and they acquire a momentum kick along the jet direction. Because the collision occurs at the early stage in the presence of the jet, the ridge provides direct information on the momentum distribution of the medium partons at the moment of jet-(medium parton) collision.

The STAR, PHENIX, and PHOBOS data for AA collisions at RHIC and the CMS data for pp collisions at LHC are consistent with the initial momentum distributions in the form of a rapidity plateau, with a thermal like transverse momentum distribution. While the functional form of the momentum distribution is the same, the longitudinal and transverse momentum at the two energies need to be properly scaled according the their differences in collision energies. The longitudinal rapidity need to be scaled according to the collider beam rapidity y_B in the center-of-mass system, and the transverse momentum distribution temperature parameters for pp collision at 7 TeV need to be scaled up by a factor of 1.4 compared to the case of $\sqrt{s_{NN}} = 0.2$ TeV, and the medium particle initial time t_0 reduced by the same factor of 1.4. This factor of 1.4 was estimated from the ratio of the average transverse momenta of pp collisions at the two different energies.

We estimate that the average number of kicked medium partons in the most central pp collisions at 7 TeV with the highest multiplicity is approximately 1.5. This is less than the number of kicked medium partons of about 4 for the most central Au-Au collisions at $\sqrt{s_{NN}} = 0.2$ TeV. The medium produced in pp collision at 7 TeV is not as dense as the medium produced in the most central AuAu collisions at $\sqrt{s_{NN}} = 0.2$ TeV, but the medium is nonetheless dense enough for the jet to kick the medium partons to turn them into ridge particles for our examination.

Using our knowledge of the physical quantities in the momentum kick model analyses for AA collisions at RHIC energies, there is only a single parameter we vary in trying to understand pp data at 7 TeV. We find that in pp collisions at 7 TeV, experimental data suggest a greater momentum kick value, $q_L = 2$ GeV/c, which is twice as large as $q_L \sim 1$ GeV/c for RHIC AA collisions at $\sqrt{s_{NN}} = 0.2$ TeV.

The ridge yields for pp collisions are more prominent in the region of $1 < p_T < 3$ GeV/c. Such a feature arises because the ridge particles are just particles whose momenta are shifted by the momentum kick. The shift of $q_L = 2$ GeV/c will place the center of the momentum distribution in the p_T region between 1 and 3 GeV/c. Hence the ridge yield is greater in this region compared to other p_T regions.

The approximate validity of the momentum kick model raises the interesting question on the nature of the scattering between the jet and the medium partons. It suggests a picture of the medium parton absorbing a part of the jet longitudinal momentum in its scattering with the jet. We can envisage that the jet at this stage is a transversely broad object in the form of a cloud of gluons propagating together in a bundle and the complete absorption of a part of the gluon cloud by the medium parton imparts the longitudinal momentum to the medium parton to carry the medium parton out to become a ridge particle. In this simple description, the jet behaves like a composite object and the scattering between the jet and the medium is not a simple two-body elastic scattering process, as in the case with a jet parton of ultrahigh p_T. It is more like "shooting a water hose on a bunch of fast-moving ping-pong balls".[2] Further theoretical and experimental investigations on the nature of the jet-(medium parton) collision for relatively low-p_T jets at this stage will be of great interest.

Transverse hydrodynamical expansion will lead to azimuthal correlations [32,33,40,41,49–51]. However, a quantitative analysis of the effects of the dynamical expansion needs to be examined carefully as the transverse flow depends sensitively on time [77] and it is much slower than the longitudinal expansion [68]. Furthermore, the transverse hydrodynamics for a fluid system with nonisotropic momentum distribution in the early history of the expansion has not been worked out in details. In the analogous case with an isotropically thermalized fluid, the picture of transverse expansion [77] reveals that soon after the stage of transverse overlap at which the jets are produced, the medium is essentially at rest with little transverse expansion. The transverse expansion commences only after the rarefaction wave passes through the medium from the outer surface inward. The time for the rarefaction waves to travel depends on the radius of the medium and the speed of the rarefaction wave which is the speed of sound. Future investigations on hydrodynamical solutions for a nonisotropic momentum distributions and azimuthally asymmetric shapes will provide a more accurate calculation of the effects of transverse flow in azimuthal correlations.

Whatever the proposed mechanism may be, collisions of the jet with the medium partons are bound to occur, and the collisional correlation between the colliding objects as discussed in the momentum kick model must be taken into account because these collisional correlations will contribute to the two-particle correlation function.

The momentum kick model provides a unifying description for ridges with or without a high-p_T trigger. The description generalizes the trigger to include high-p_T and low-p_T particles due to the fact that jet fragments are found in high p_T as well as in low p_T. Many peculiar and puzzling features of the minimum-bias correlation data of the STAR Collaboration [4,16,18,54] find simple explanations in the momentum kick model. If we limit our attention to the near side, the case with a high-p_T trigger involves mainly NJF-NJF and NJF-NKMP correlations while the case of minimum-bias pair correlation with low-p_T triggers involves not only these NJF-NJF and NJF-NKMP correlations but also the NKMP-NKMP correlation. The additional NKMP-NKMP correlation in the low-p_T trigger case will contribute only when more than one medium partons are kicked by the same jet and will be important in the ridge region. In extended dense medium as occurs in heavy-ion collisions, the number of partons kicked

[2]The author thanks Dr. R. L. Ray for such a colorful description of the momentum kick model.

by the same jet becomes considerable and this NKMP-NKMP contribution should be appropriately taken into account.

In conclusion, the ridges in both AA collisions at $\sqrt{s_{NN}} = 0.2$ TeV and pp collisions at 7 TeV in LHC can be described by the same mechanism of the momentum kick model involving the collision of jets with medium partons. The momentum distributions of the medium partons at the moment of jet-(medium parton) collisions have similar features of a rapidity plateau and a thermal type transverse momentum distribution.

For pp collisions at 7 TeV, it will be of interest to carry out measurements of the (p_{T1}, p_{T2}) correlations with a minimum-bias trigger that will reveal whether there is a correlation at $p_{T1} \sim p_{T2} \sim 2$ GeV, as suggested by the results of Fig. 7 and similar to the correlation of $p_{T1} \sim p_{T2} \sim 1$ GeV/c for pp collisions at 0.2 TeV. Future experiments also call for the measurement of the p_T distribution of various components with a high-p_T trigger to separate out different correlation contributions. Further acquisitions of more correlation data of the ridge yields, in large regions of the phase space in different phase space cuts and combinations, will provide useful information on the correlation mechanism and the momentum distribution of medium partons at the early history of the collision.

ACKNOWLEDGMENTS

The authors thank Drs. Vince Cianciolo and R. L. Ray for helpful discussions. This research was supported in part by the Division of Nuclear Physics, US Department of Energy.

[1] CMS Collaboration, V. Khachatryan *et al.*, J. High Energy Phys. 09 (2010) 091.
[2] CMS Collaboration, arXiv:1105.2438 (2011).
[3] J. Adams *et al.*, for the STAR Collaboration, Phys. Rev. Lett. **95**, 152301 (2005).
[4] J. Adams *et al.* (STAR Collaboration), Phys. Rev. C **73**, 064907 (2006).
[5] J. Putschke (STAR Collaboration), J. Phys. G **34**, S679 (2007).
[6] J. Bielcikova (STAR Collaboration), J. Phys. G **34**, S929 (2007).
[7] F. Wang (STAR Collaboration), Invited talk at the XIth International Workshop on Correlation and Fluctuation in Multiparticle Production, Hangzhou, China, November 2007, Int. J. Mod. Phys. E **10**, 3168 (2007).
[8] J. Bielcikova (STAR Collaboration), J. Phys. G **34** S929 2007; for the STAR Collaboration, talk presented at the 23rd Winter Workshop on Nuclear Dynamics, Big Sky, Montana, USA, February 11–18, 2007 arXiv:0707.3100; for the STAR Collaboration, talk presented at the XLIII Rencontres de Moriond, QCD and High Energy Interactions, La Thuile, March 8–15, 2008 arXiv:0806.2261.
[9] B. Abelev (STAR Collaboration), talk presented at the 23rd Winter Workshop on Nuclear Dynamics, Big Sky, Montana, USA, February 11–18, 2007 arXiv:0705.3371.
[10] L. Molnar (STAR Collaboration), J. Phys. G **34**, S593 (2007).
[11] R. S. Longacre (STAR Collaboration), Int. J. Mod. Phys. E **16**, 2149 (2007).
[12] C. Nattrass (STAR Collaboration), J. Phys. G **35**, 104110 (2008).
[13] A. Feng (STAR Collaboration), J. Phys. G **35**, 104082 (2008).
[14] P. K. Netrakanti (STAR Collaboration), J. Phys. G **35**, 104010 (2008).
[15] O. Barannikova (STAR Collaboration), J. Phys. G **35**, 104086 (2008).
[16] M. Daugherity (STAR Collaboration), J. Phys. G **35**, 104090 (2008).
[17] M. van Leeuwen (STAR Collaboration), Eur. Phys. J. C **61**, 569 (2009).
[18] T. A. Trainor, Phys. Rev. C **78**, 064908 (2008); T. A. Trainor and D. T. Kettler, Phys. Rev. D **74**, 034012 (2006); T. A. Trainor, Phys. Rev. C **80**, 044901 (2009); J. Phys. G **37**, 085004 (2010).
[19] A. Adare, *et al.* (PHENIX Collaboration), Phys. Rev. C **78**, 014901 (2008).
[20] M. P. McCumber (PHENIX Collaboration), J. Phys. G **35**, 104081 (2008).
[21] Chin-Hao Chen (PHENIX Collaboration), Hard Probes 2008 International Conference on Hard Probes of High Energy Nuclear Collisions, A Toxa, Galicia, Spain, June 8–14, 2008.
[22] Jiangyong Jia (PHENIX Collaboration), J. Phys. G **35**, 104033 (2008).
[23] M. J. Tannenbaum, Eur. Phys. J. C **61**, 747 (2009).
[24] E. Wenger (PHOBOS Collaboration), J. Phys. G **35**, 104080 (2008).
[25] C. Y. Wong, Phys. Rev. C **76**, 054908 (2007).
[26] C. Y. Wong, Chin. Phys. Lett. **25**, 3936 (2008).
[27] C. Y. Wong, J. Phys. G **35**, 104085 (2008).
[28] C. Y. Wong, Phys. Rev. C **78**, 064905 (2008).
[29] C. Y. Wong, Phys. Rev. C **80**, 034908 (2009).
[30] C. Y. Wong, Phys. Rev. C **80**, 054917 (2009).
[31] C. Y. Wong, Nonl. Phen. Compl. Syst. **12**, 315 (2009).
[32] E. Shuryak, Phys. Rec. C **76**, 047901 (2007).
[33] S. A. Voloshin, Nucl. Phys. A **749**, 287 (2005).
[34] C. B. Chiu and R. C. Hwa, Phys. Rev. C **79**, 034901 (2009).
[35] R. C. Hwa and C. B. Yang, Phys. Rev. C **67**, 034902 (2003); R. C. Hwa and Z. G. Tan, *ibid.* **72**, 057902 (2005); R. C. Hwa and C. B. Yang, arXiv:nucl-th/0602024.
[36] C. B. Chiu and R. C. Hwa, Phys. Rev. C **72**, 034903 (2005).
[37] R. C. Hwa, Phys. Lett. B **666**, 228 (2008).
[38] V. S. Pantuev, arXiv:0710.1882.
[39] A. Dumitru, F. Gelis, L. McLerran, and R. Venugopalan, Nucl. Phys. A **810**, 91 (2008).
[40] S. Gavin and G. Moschelli, J. Phys. G **35**, 104084 (2008).
[41] S. Gavin, L. McLerran, and G. Moschelli, Phys. Rev. C **79**, 051902 (2009).
[42] N. Armesto, C. A. Salgado, and U. A. Wiedemann, Phys. Rev. Lett. **93**, 242301 (2004).
[43] P. Romatschke, Phys. Rev. C **75**, 014901 (2007).
[44] A. Majumder, B. Muller, and S. A. Bass, Phys. Rev. Lett. **99**, 042301 (2007).
[45] A. Dumitru, Y. Nara, B. Schenke, and M. Strickland, Phys. Rev. C **78**, 024909 (2008); B. Schenke, A. Dumitru, Y. Nara, and M. Strickland, J. Phys. G **35**, 104109 (2008).
[46] R. Mizukawa, T. Hirano, M. Isse, Y. Nara, and A. Ohnishi, J. Phys. G **35**, 104083 (2008).
[47] Jianyong Jia and R. Lacey, Phys. Rev. C **79**, 011901 (2009).
[48] Jianyong Jia, Eur. Phys. J. C **61**, 255 (2009).

[49] Y. Hama, R. P. G. Andrade, F. Grassi, and W.-L. Qian, talk presented at ISMD2010, 21–25 September, 2010, University of Antwerp (Belgium).
[50] A. Dumitru, K. Dusling, F. Gelis, J. Jalilian-Marian, T. Lappi, and R. Venugopalan, Phys. Lett. B **697**, 21 (2011).
[51] K. Werner, Iu. Karpenko, K. Mikhailov, and T. Pierog, arXiv:1104.3269.
[52] R. C. Hwa and C. B. Yang, Phys. Rev. C **83**, 024911 (2011).
[53] C. B. Chiu and R. C. Hwa, arXiv:1012.3486.
[54] T. A. Trainor, arXiv:1008.4757; arXiv:1011.6351; arXiv:1012.2373.
[55] T. A. Trainor and D. T. Kettler, Phys. Rev. C **83**, 034903 (2011).
[56] B. A. Arbuzov, E. E. Boos, and V. I. Savrin, arXiv:1104.1283.
[57] M. Yu. Azarkin, I. M. Dremin, and A. V. Leonidov, arXiv:1102.3258.
[58] H. R. Grigoryan and Y. V. Kovchegov, arXiv:1012.5431.
[59] I. Bautista, J. Dias de Deus, and C. Pajares, arXiv:1011.1870.
[60] I. O. Cherednikov and N. G. Stefanis, arXiv:1010.4463.
[61] I. M. Dremin and V. T. Kim, arXiv:1010.0918.
[62] E. Levin and A. H. Rezaeian arXiv:1105.3275.
[63] T. A. Trainor and D. T. Kettler, arXiv:1010.3048.
[64] T. A. Trainor and R. L. Ray, arXiv:1105.5428; R. L. Ray, arXiv:1106.5023.
[65] C. Y. Wong, *Introduction to High-Energy Heavy Ion Collisions* (World Scientific, Singapore, 1994).
[66] T. T. Chou and C. N. Yang, Phys. Rev. **170**, 1591 (1968); Phys. Lett. B **135**, 175 (1984).
[67] J. D. Bjorken, Phys. Rev. D **27**, 140 (1983).
[68] L. D. Landau, Izv. Akad. Nauk SSSR **17**, 51 (1953); S. Z. Belenkij and L. D. Landau, Usp. Fiz. Nauk **56**, 309 (1955) [Nuovo Cimento, Suppl. **3**, 15 (1956)].
[69] C. Y. Wong, Phys. Rev. C **78**, 054902 (2008).
[70] C. Y. Wong, lectures presented at the Helmholtz International Summer School, Bogoliubov Laboratory of Theoretical Physics, JINR, Dubna, July 14–26, 2008.
[71] M. Basile *et al.*, Nuovo Cimento A **65**, 400 (1981); M. Basile, *ibid.* **67**, 244 (1981).
[72] U. W. Heinz and P. F. Kolb, Nucl. Phys. A **702**, 269 (2002).
[73] V. Khachatryan *et al.* (CMS Collaboration), Phys. Rev. Lett. **105**, 022002 (2010).
[74] A. Casher, J. Kogut, and L. Susskind, Phys. Rev. D **10**, 732 (1974).
[75] C. Y. Wong, R. C. Wang, and C. C. Shih, Phys. Rev. D **44**, 257 (1991).
[76] K. Nakamura *et al.* (Particle Data Group), J. Phys. G **37**, 075021 (2010)
[77] G. Baym, B. L. Friman, J.-P. Blaizot, M. Soyeur, and W. Czyz, Nucl. Phys. A **407**, 541 (1983).